Fault-Tolerant Control of Magnetic Levitation System Based on State Observer in High Speed Maglev Train

MINGDA ZHAI , ZHIQIANG LONG, AND XIAOLONG LI
National University of Defense Technology, Changsha 410073, China

Corresponding author: Zhiqiang Long (lzq@maglev.cn)

ABSTRACT In recent years, the high-speed rail train has achieved great progress, but the wheel–rail relationship and the catenary–pantograph relationship are the bottlenecks to further increase the speed. The maglev train is an entirely new mode of transport without wheels. It takes full advantage of electromagnetic force to achieve active levitation and runs the train by the linear motor. It completely abandons the frictional resistance to speed up over 500 km/h practically. The redundancy and fault tolerance of the magnetic levitation system, which is considered as the wheels of the high-speed maglev train, play a major role in the safety and reliability of high-speed maglev train. However, due to the failure of sensors and the existence of track seams, the suspension unit often breaks down. The performance of suspension join-structure under the modular redundancy strategy with sensor failure is analyzed and investigated. The investigation carried out by us reveals that the overall performance is unpleasant and the electromagnet fevers seriously. In order to solve this problem, we propose and design the state observer as a solution to construct the fault-tolerant control system. The designed observer is applied to estimate the gap measurement of the fault sensor so that the suspension unit will not fail. Therefore, The fault-tolerant control system based on state observer improves the redundancy and fault tolerance capacity of the magnetic levitation system with sensor failure significantly.

INDEX TERMS High speed maglev train, magnetic levitation system, sensor, fault-tolerant, observer.

I. INTRODUCTION

Ever since the first steam locomotive was invented in England, the wheel-rail train has never stopped to carry passengers all over the world [1]. With the increasing expectation of train speed, the high speed rail has been of considerable interest to the whole society in recent years. In the process of rapid development, China is seated at the forefront of the world's high speed railway development. There are more than twice as many high-speed trains in China as the rest of the world combined. The Chinese high-speed rail technology has already been China's global calling card. In September 2017, Fuxing Hao EMU took the lead in realizing 350 km/h operation on Beijing-Shanghai high-speed railway, and China has become the fastest commercial operation country in the world. Great progress has been made in this field, but the

wheel-rail relationship and the catenary-pantograph relationship of conventional wheel-rail trains are the bottleneck to further increase the speed. The maglev train is an entirely new mode of transport without wheels. It takes full advantage of electromagnetic force to achieve active levitation and runs the train by the linear motor [2], [3]. It completely abandons the frictional resistance speed up over 500 km/h practically. In 2003, Shanghai high speed maglev created and still maintains the world railway commercial speed record of 431 km/h. The superconducting maglev train of Japan will run in 2027 at the high speed of 600 km/h.

Moreover, the Incheon airport maglev of South Korea, the Changsha maglev express line and the Beijing S1 line have been operated one after another in recent years. Maglev train has received considerably increasing attention and been an active traffic field. Experts and scholars agree that the maglev technology has already been fully developed and matured. Therefore, National Key R & D Program of China

---

The associate editor coordinating the review of this manuscript and approving it for publication was Muhammad Awais Javed.

FIGURE 1. The photograph of high-speed maglev train in Shanghai.

FIGURE 2. The illustration of suspension join- structure.

"maglev traffic system key technology" is officially established to increase the speed up to 600 km/h. However, a great number of fundamental technical problems still need to be studied and investigated.

This subject is concerned chiefly with the study of the magnetic levitation system in high speed maglev train. The magnetic levitation system plays a significant role in suspending the maglev train above the rail against the gravity. The safety and reliability issues on magnetic levitation system are actually the most critical factors for the high speed maglev train. However, the sensor of magnetic levitation system has a high failure rate because it works at a high-temperature, high-magnetic and high-vibration environment. Even though the concept of modular redundancy is employed, the suspension unit often breaks down due to sensor failure and seams in the track. It will have a dreadful effect on the overall performance of magnetic levitation system, and lead to electromagnet fever seriously [4], [5]. The problem I have referred to falls within the field of fault-tolerant control of magnetic levitation system [6]–[8].

In this paper, we propose and design a observer as a solution to address this problem. When the sensor fails, the gap value will be obtained by the designed observer effectively and accurately. The fault-tolerant control system is constructed to improve the redundancy capacity of magnetic levitation system with sensor failure.

II. MAGNETIC LEVITATION SYSTEM OF HIGH SPEED MAGLEV

As we all know, magnets of the same polarity repel each other, while those of different polarity attract each other. The high speed maglev train makes full use of the attraction between the electromagnet and the long stator track to achieve suspension at a desired gap. A complete high speed maglev train has 32 sets of suspension unit. When the current is switched on, the upward electromagnetic force is generated. Therefore, the high maglev train can suspend in the air against the gravity. The balance between the gravity and electromagnetic force will always be achieved.

The magnetic levitation system of high-speed maglev train adopts a unique join-structure, and two arms of the corbel are rigid connected. Two adjacent suspension units and corbel are connected by metal rubber springs to form the whole
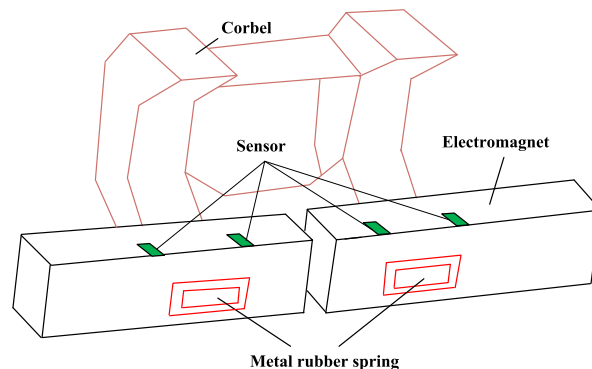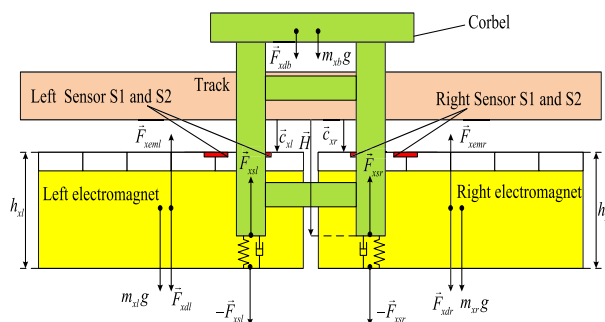

FIGURE 3. The model of suspension join-structure.

suspension join-structure. The metal rubber spring is able to generate relative displacement and reduce the degree of coupling. The illustration of suspension join-structure is presented in the Fig. 2.

As shown in the Fig. 2, the suspension join-structure is a large system in which two suspension units and corbel system are coupled to each other. The establishment of mathematical model must take the whole join-structure into consideration.

The gap of the left electromagnet is $\vec{c}_{xl}$, and the right electromagnet is $\vec{c}_{xr}$; the external interference force on the left electromagnet is $\vec{F}_{xdl}$, and the right is $\vec{F}_{xdr}$; the height and mass of the left electromagnet is h_{xl} and m_{xl} respectively; the right is h_{xr} and m_{xr}; the natural length, stiffness and damping of the left metal rubber spring is l_{xl0}, k_{xl} and η_{xl} respectively; the right is l_{xr0}, k_{xr} and η_{xr}; the voltage and current of the left electromagnet is u_{xcl} and i_{xl} respectively; the electromagnetic force is $\vec{F}_{xeml}$ and the restoring force of the metal rubber spring acting upon the corbel is $\vec{F}_{xsl}$; the right is u_{xcr}, i_{xr}, $\vec{F}_{xemr}$, $\vec{F}_{xsr}$ respectively; the equivalent mass of the upper bogie is m_{xb} and the suffered interference force is $\vec{F}_{xdb}$; the displacement of the lower edge of the corbel to the lower surface of the maglev track is $\vec{H}$; the number of turns, the resistance, the polar area and the permeability of vacuum is N_x, R_x, A_x and μ_0 respectively. Thus, the mathematical model of magnetic levitation system is established as follows:

$$u_{xcl}(t) = R_x i_{xl}(t) + \frac{d}{dt}\left(\frac{N_x^2 i_{xl}(t)}{2c_{xl}(t)/\mu_0 A_x}\right) \quad (1)$$

$$u_{xcr}(t) = R_x i_{xr}(t) + \frac{d}{dt}\left(\frac{N_x^2 i_{xr}(t)}{2c_{xr}(t)/\mu_0 A_x}\right) \quad (2)$$

$$F_{xeml}(i_{xl}, c_{xl}) = \frac{\mu_0 N_x^2 A_x}{4}\left[\frac{i_{xl}}{c_{xl}}\right]^2 \quad (3)$$

$$F_{xemr}(i_{xr}, c_{xr}) = \frac{\mu_0 N_x^2 A_x}{4}\left[\frac{i_{xr}}{c_{xr}}\right]^2 \quad (4)$$

$$F_{xsl} = k_{xl}[l_{xl0} - (c_{xl} + h_{xl} - H)]$$
$$- \eta_{xl}[\dot{c}_{xl}(t) - \dot{H}(t)] \quad (5)$$

$$F_{xsr} = k_{xr}[l_{xr0} - (c_{xr} + h_{xr} - H)]$$
$$- \eta_{xr}[\dot{c}_{xr}(t) - \dot{H}(t)] \quad (6)$$

$$m_{xl}\ddot{c}_{xl} = m_{xl}g + F_{xsl} + F_{xdl} - F_{xeml} \quad (7)$$

$$m_{xr}\ddot{c}_{xr} = m_{xr}g + F_{xsr} + F_{xdr} - F_{xemr} \quad (8)$$

$$m_{xb}\ddot{H} = m_{xb}g + F_{xdb} - F_{xsl} - F_{xsr} \quad (9)$$

The linearization of the above equations is accomplished near the working point. Thus, the state variables of linearization system are specified, and the state space equation of linearization system is defined:

$$\mathbf{x_{xl}} = \begin{pmatrix} c_{xl} & \dot{c}_{xl} & i_{xl} \end{pmatrix}^T, \quad \mathbf{x_{xr}} = \begin{pmatrix} c_{xr} & \dot{c}_{xr} & i_{xr} \end{pmatrix}^T$$

$$\mathbf{u_{xl}} = \begin{pmatrix} u_{xcl} & F_{xdl} \end{pmatrix}^T, \quad \mathbf{u_{xr}} = \begin{pmatrix} u_{xcr} & F_{xdr} \end{pmatrix}^T,$$

$$\mathbf{u_{xb}} = F_{xdb} \quad y_{xl} = c_{xl}, \quad y_{xr} = c_{xr}, \quad y_{xb} = H$$

$$\mathbf{x_{xl}} = \begin{pmatrix} c_{xl} & \dot{c}_{xl} & i_{xl} \end{pmatrix}^T, \quad \mathbf{x_{xr}} = \begin{pmatrix} c_{xr} & \dot{c}_{xr} & i_{xr} \end{pmatrix}^T$$

$$\begin{cases} \begin{pmatrix} \dot{\mathbf{x}}_{\mathbf{xl}} \\ \dot{\mathbf{x}}_{\mathbf{xr}} \\ \dot{\mathbf{x}}_{\mathbf{xb}} \end{pmatrix} = \begin{pmatrix} \mathbf{A_{xl}} & \mathbf{0} & \mathbf{A_{xlb}} \\ \mathbf{0} & \mathbf{A_{xr}} & \mathbf{A_{xrb}} \\ \mathbf{A_{xbl}} & \mathbf{A_{xbr}} & \mathbf{A_{xb}} \end{pmatrix} \begin{pmatrix} \mathbf{x_{xl}} \\ \mathbf{x_{xr}} \\ \mathbf{x_{xb}} \end{pmatrix} \\ \quad + \begin{pmatrix} \mathbf{B_{xl}} & & \\ & \mathbf{B_{xr}} & \\ & & \mathbf{B_{xb}} \end{pmatrix} \begin{pmatrix} \mathbf{u_{xl}} \\ \mathbf{u_{xr}} \\ \mathbf{u_{xb}} \end{pmatrix} \\ \begin{pmatrix} \mathbf{y_{xl}} \\ \mathbf{y_{xr}} \\ \mathbf{y_{xb}} \end{pmatrix} = \begin{pmatrix} \mathbf{C_{xs}} & & \\ & \mathbf{C_{xs}} & \\ & & \mathbf{C_{xb}} \end{pmatrix} \begin{pmatrix} \mathbf{x_{xl}} \\ \mathbf{x_{xr}} \\ \mathbf{x_{xb}} \end{pmatrix} \end{cases}$$
$$(10)$$

where:

$$\mathbf{A_{xl}} = \begin{pmatrix} 0 & 1 & 0 \\ \dfrac{k_{xzl} - k_{xl}}{m_{xl}} & -\dfrac{\eta_{xl}}{m_{xl}} & -\dfrac{k_{xil}}{m_{xl}} \\ 0 & \dfrac{k_{xil}}{L_{xl0}} & -\dfrac{R_x}{L_{xl0}} \end{pmatrix}$$

$$\mathbf{A_{xr}} = \begin{pmatrix} 0 & 1 & 0 \\ \dfrac{k_{xzr} - k_{xr}}{m_{xr}} & -\dfrac{\eta_{xr}}{m_{xr}} & -\dfrac{k_{xir}}{m_{xr}} \\ 0 & \dfrac{k_{xir}}{L_{xr0}} & -\dfrac{R_x}{L_{xr0}} \end{pmatrix}$$

$$\mathbf{A_{xb}} = \begin{pmatrix} 0 & 1 \\ -\dfrac{k_{xl} + k_{xr}}{m_{xb}} & -\dfrac{\eta_{xl} + \eta_{xr}}{m_{xb}} \end{pmatrix}$$

$$\mathbf{A_{xlb}} = \begin{pmatrix} 0 & 0 \\ \dfrac{k_{xl}}{m_{xl}} & \dfrac{\eta_{xl}}{m_{xl}} \\ 0 & 0 \end{pmatrix}$$
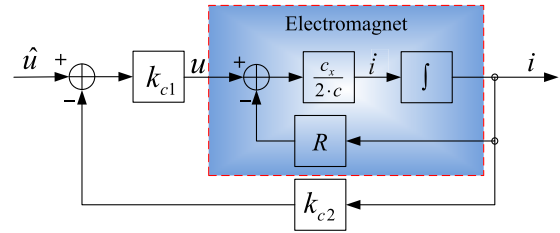

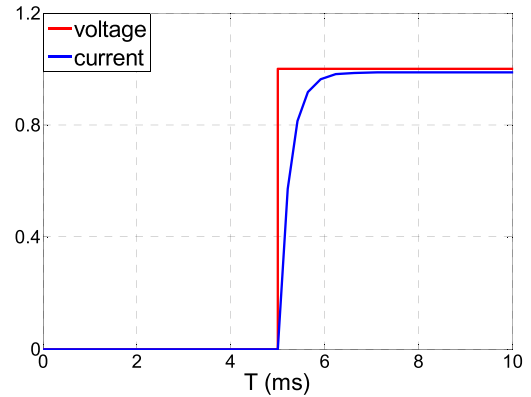**FIGURE 4.** The schematic diagram of current loop.

FIGURE 5. The response of electromagnet using current loop feedback.

$$\mathbf{A_{xbl}} = \begin{pmatrix} 0 & 0 & 0 \\ \dfrac{k_{xl}}{m_{xb}} & \dfrac{\eta_{xl}}{m_{xb}} & 0 \end{pmatrix} \quad \mathbf{A_{xbr}} = \begin{pmatrix} 0 & 0 & 0 \\ \dfrac{k_{xr}}{m_{xb}} & \dfrac{\eta_{xr}}{m_{xb}} & 0 \end{pmatrix}$$

$$\mathbf{B_{xl}} = \begin{pmatrix} 0 & 0 \\ 0 & \dfrac{1}{m_{xl}} \\ \dfrac{1}{L_{xl0}} & 0 \end{pmatrix} \quad \mathbf{B_{xr}} = \begin{pmatrix} 0 & 0 \\ 0 & \dfrac{1}{m_{xr}} \\ \dfrac{1}{L_{xr0}} & 0 \end{pmatrix}$$

$$\mathbf{B_{xb}} = \dfrac{1}{m_{xb}}, \quad \mathbf{C_{xs}} = (100) \quad \text{and} \quad \mathbf{C_{xb}} = (10)$$

The controllability of the magnetic levitation system is determined by achieving and analyzing the rank of the controllability matrix.

$$rank([B\ AB\ A^2B\ A^3B\ A^4B\ A^5B]) = 6 \quad (11)$$

Therefore, the magnetic levitation system is completely controllable. By designing a perfect controller, the magnetic levitation system is able to work steadily in the desired state.

The electromagnet is a typical inertia link, and the current response is seriously lagged behind the voltage change. The response time is not able to meet the demand of high speed maglev train. Therefore, the current feedback method is adopted to reduce the response time. The schematic diagram of current loop feedback is illustrated in the Fig. 4. The proper selection of parameters is able to reduce the response time of electromagnet down to 10 milliseconds, which is shown in the Fig. 5. What's more, the current feedback also make the system change from 8-order to 6-order.

TABLE 1. Parameter list of magnetic levitation system.

Symbol	Meaning	Quantity	Unit
m_{xl}	Mass of left electromagnet	300	kg
m_{xr}	Mass of right electromagnet	300	kg
m_{xb}	Equivalent mass of suspension frame	450	kg
R_x	Resistance	3.84	Ω
N_x	Number of turns	270	
μ_0	vacuum permeability	$4\pi \times 10^{-7}$	
c_{x0}	set gap	12	mm

The parameters of the magnetic levitation system are indicated in Table. 1.

These parameters are brought into the model of magnetic levitation system, and the state space equation after order-reduction is obtained:

$$
\begin{cases}
\dot{\mathbf{x}} = \begin{pmatrix}
0 & 1 & 0 & 0 & 0 & 0 \\
\dfrac{171000}{3} & 0 & 0 & 0 & \dfrac{200000}{3} & 0 \\
0 & 0 & 0 & 1 & 0 & 0 \\
0 & 0 & \dfrac{171000}{3} & 0 & \dfrac{200000}{3} & 0 \\
0 & 0 & 0 & 0 & 0 & 1 \\
\dfrac{2000000}{45} & 0 & \dfrac{2000000}{45} & 0 & -\dfrac{4000000}{45} & 0
\end{pmatrix} \mathbf{x} \\
\quad + \begin{pmatrix}
0 & 0 \\
-4.13 & 0 \\
0 & 0 \\
0 & -4.13 \\
0 & 0 \\
0 & 0
\end{pmatrix} \mathbf{u} \\
\mathbf{y} = \begin{pmatrix}
1 & 0 & 0 & 0 & 0 & 0 \\
0 & 0 & 1 & 0 & 0 & 0
\end{pmatrix} \mathbf{x}
\end{cases}
\tag{12}
$$

where:

$$\mathbf{u} = \begin{pmatrix} u_{xcl} & u_{xcr} \end{pmatrix}^T, \quad \mathbf{x} = \begin{pmatrix} c_{xl} & \dot{c}_{xl} & c_{xr} & \dot{c}_{xr} & H & \dot{H} \end{pmatrix}^T$$

According to Eq. 12, it is found that the magnetic levitation system is a typical multi-input multi-output system. Consequently, the method of quadratic optimal control is adopted to design a full-state feedback controller. The feedback parameters of controller is obtained:

$$\mathbf{K} = \begin{pmatrix}
-6130 & -1001 & -5771 & -1.4 & 1470 & -2.2 \\
-5771 & -1.4 & -6130 & -1001 & 1470 & -2.2
\end{pmatrix}$$

In order to examine the performance of the designed controller, the designed control algorithm is directly substituted into the nonlinear model of the magnetic levitation system. The initial gap is set to 20 mm and the target gap is set to 12 mm. When the floating instruction is issued, the response of the suspension join-structure is observed.
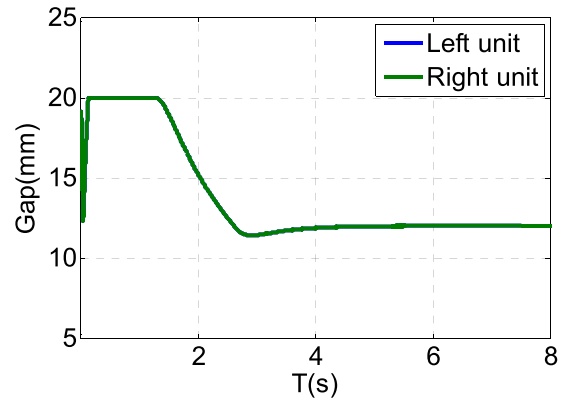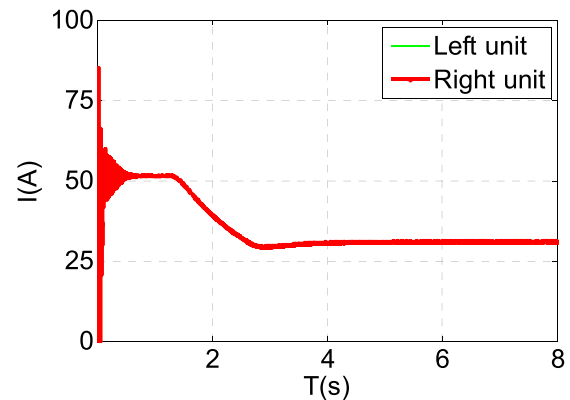
FIGURE 6. The response of suspension join-structure. (a) The gap of left and right unit. (b) The current of left and right unit.

As described in Fig. 6, the left and right unit began to rise slowly and eventually fixed at the set gap 12 mm. There is no obvious fluctuation in the whole process, and the system overshoot and response time are within a reasonable range. The simulation result shows the designed controller is qualified.

III. MODULAR REDUNDANCY STRATEGY FOR SUSPENSION JOIN-STRUCTURE WITH SENSOR FAILURE

The magnetic levitation system has three key components: suspension controller, sensor and electromagnet. We will consequently refer to it as a suspension unit. The suspension join-structure composes of two suspension units to provide mutual redundancy function. Once a suspension unit is invalid, another suspension unit is still able to work normally and levitate the whole suspension join-structure. The suspension unit also consists of two sensors to provide mutual redundancy function. Sensors measure the gap between the electromagnet and the long stator track in real time. The suspension controller receives the gap signals and calculates the control quantity to adjust the position of electromagnet.

The long stator track of high-speed maglev train consists of several functional parts. The length of the functional parts system is 3.096 m, so there will be a seam every 3.096 m.
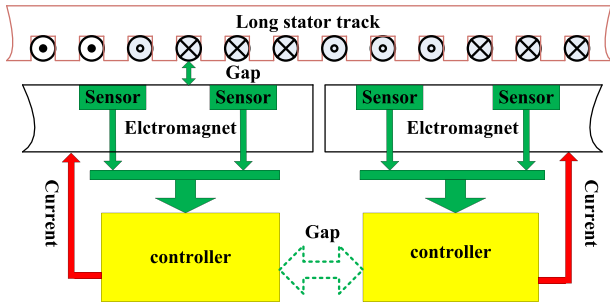
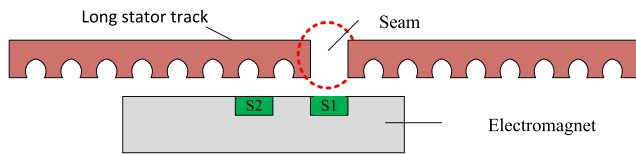**FIGURE 7.** The modular redundancy strategy for suspension join-structure.

FIGURE 8. The illustration of the sensors passing through the seam.

**TABLE 2.** The effects of sensor failure on the suspension unit.

| Left side		Right side		Join-structure	
S1	S2	S1	S2	Left unit	Right unit
Y	Y	Y	Y	Y	Y
-	N	Y	Y	N	Y
N	-	Y	Y	N	Y
Y	Y	-	N	Y	N
Y	Y	N	-	Y	N
N	-	-	N	N	N
N	-	N	-	N	N
-	N	N	-	N	N
N	-	N	-	N	N

Y: work; N: failure; -: random

Therefore, there are many seams in the track, which cause the saturation of sensor measurement at the seams. The sensor will fail to provide true gap data of the high speed train at this moment. As shown in the Fig. 8, when the sensor S1 is located below the seam, the gap measurement is false and useless. The mutual redundancy between sensor S1 and sensor S2 is invalid. Once the sensor S2 fails, the suspension controller will not be able to achieve the gap measurement at this moment and this suspension unit will break down due to one sensor failure.

In order to discuss the effects of sensor failure on the suspension unit, we conduct a series of analysis and investigations. The following table 2 is summarized.

It is concluded that the suspension unit will be invalid only if one of two sensors fails. At this moment, the suspension join-structure relies on the adjacent suspension unit. The response of suspension join-structure with sensor failure needs to be further discussed and analyzed, which plays an
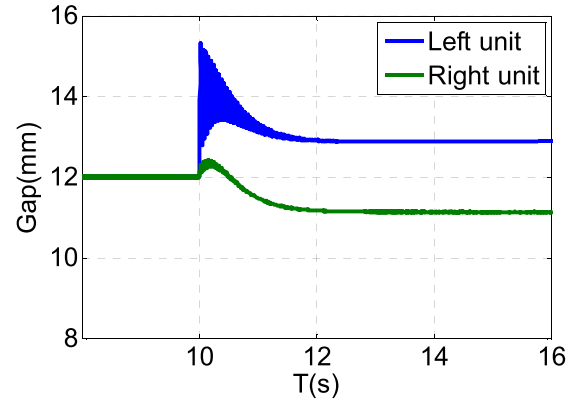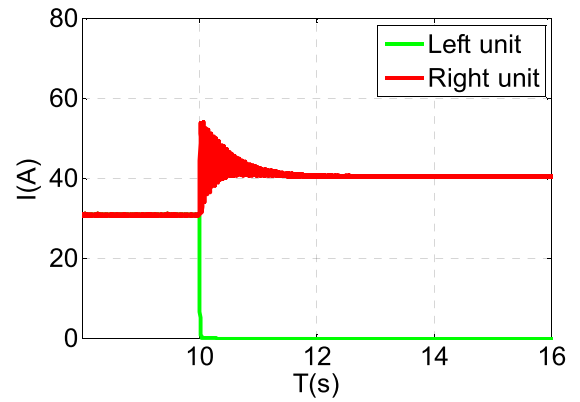
FIGURE 9. The response of suspension join-structure when the left unit is failure. (a) The gap of left and right unit. (b) The current of left and right unit.

important role in the safety and comfort of high speed maglev train.

When the left suspension unit fails due to the sensor failure, the response of suspension join-structure is observed in Fig. 9.

In order to have an overall evaluation of the modular redundancy strategy for suspension join-structure with sensor failure, the following cases are verified:

1) The left unit suffered from a step interference force of 10 kN for 3 seconds;
2) The right unit suffered from a step interference of 10 kN for 3 seconds;
3) The right unit receives a step interference with an amplitude of 2 mm for 1 second.

The system responses in these three cases is described in Fig. 10- Fig. 13.

The performance of suspension join-structure under the modular redundancy strategy with sensor failure is achieved completely. The investigation carried out by us has acquired a great number of significant conclusions:

1. When the left suspension unit fails, the right suspension unit is able to levitate the whole join-structure. However, the current of right unit becomes higher to cause electromagnet fever seriously.

2. The gap of left unit becomes larger while the right becomes smaller. They do not stabilize in the desired gap.
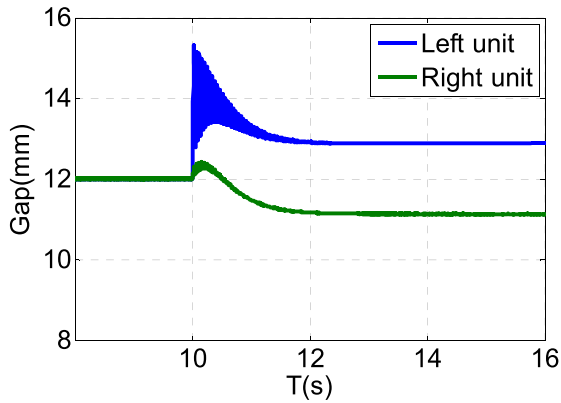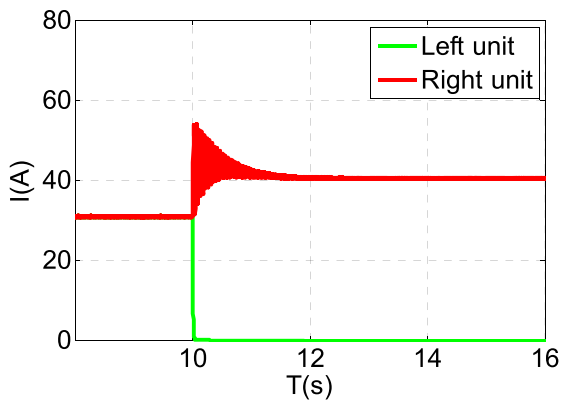
FIGURE 10. The response of suspension join-structure when the left unit is failure. (a) The gap of left and right unit. (b) The current of left and right unit.

FIGURE 11. The response of suspension join-structure when a step disturbance force of 10kN for 3 seconds on the left unit. (a) The gap of left and right unit. (b) The current of left and right unit.

The fluctuation of gap is extremely drastic under the action of disturbance forces, and the electromagnet is prone to collide the long stator track.
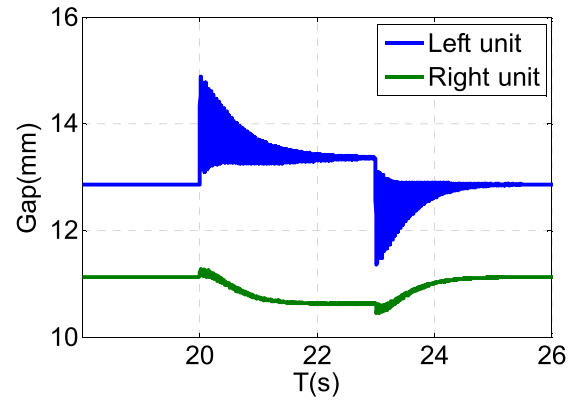
3. The modular redundancy strategy with sensor failure causes a decrease in the overall performance of suspension join-structure.

The research we have done suggests that the modular redundancy strategy with sensor failure is only functional but not satisfied. Therefore, the new redundancy strategy is necessary need to be proposed and designed to improve the fault-tolerant capacity.
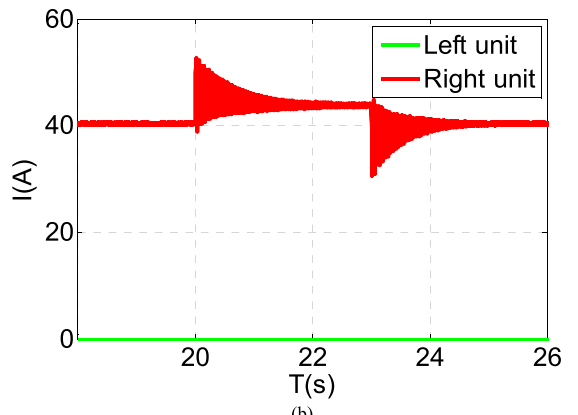
IV. DESIGN FOR STATE OBSERVER OF SUSPENSION JOIN-STRUCTURE WITH SENSOR FAILURE

The previous work is proved that the modular redundancy strategy with sensor failure causes a decrease in the overall performance of suspension join-structure. Once one of the two sensors fails, the other sensor will not be able to pass through seams and the gap measurement of this side will fail completely. Consequently, this suspension unit will break down.

In order to achieve the gap signal and reduce the probability of suspension unit failure, we propose and design the state observer as a solution to address this problem [9]–[12].

When the sensor fails, the gap measurement will be estimated by the designed observer effectively and accurately.

Without losing generality, it is assumed that the left gap measurement is unworkable. In this case, the system is featured by double input and single output. The state equation of the system is become:

$$
\begin{cases}
\dot{\mathbf{x}} = \begin{pmatrix}
0 & 1 & 0 & 0 & 0 & 0 \\
\dfrac{171000}{3} & 0 & 0 & 0 & \dfrac{200000}{3} & 0 \\
0 & 0 & 0 & 1 & 0 & 0 \\
0 & 0 & \dfrac{171000}{3} & 0 & \dfrac{200000}{3} & 0 \\
0 & 0 & 0 & 0 & 0 & 1 \\
\dfrac{2000000}{45} & 0 & \dfrac{2000000}{45} & 0 & -\dfrac{4000000}{45} & 0
\end{pmatrix} \mathbf{x} \\
\quad + \begin{pmatrix}
0 & 0 \\
-4.13 & 0 \\
0 & 0 \\
0 & -4.13 \\
0 & 0 \\
0 & 0
\end{pmatrix} \mathbf{u} \\
\mathbf{y} = \begin{pmatrix} 0 & 0 & 1 & 0 & 0 & 0 \end{pmatrix} \mathbf{x}
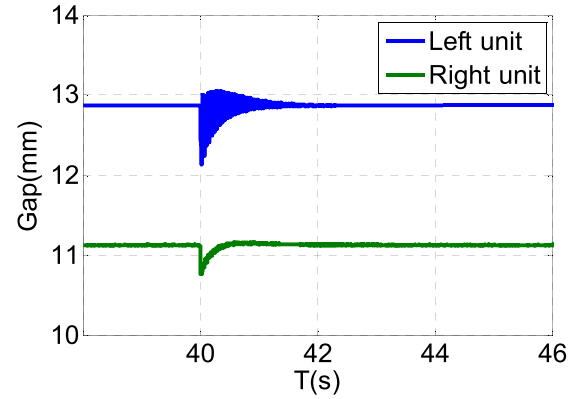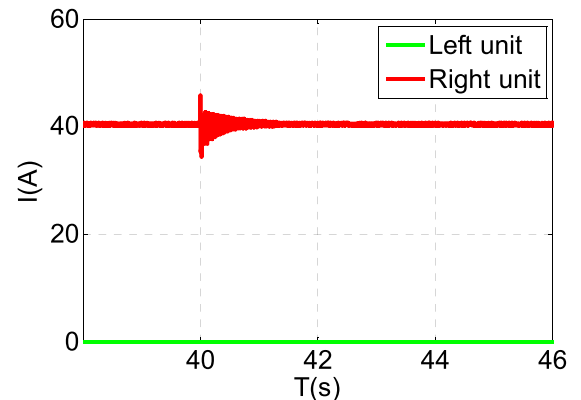\end{cases}
\tag{13}
$$
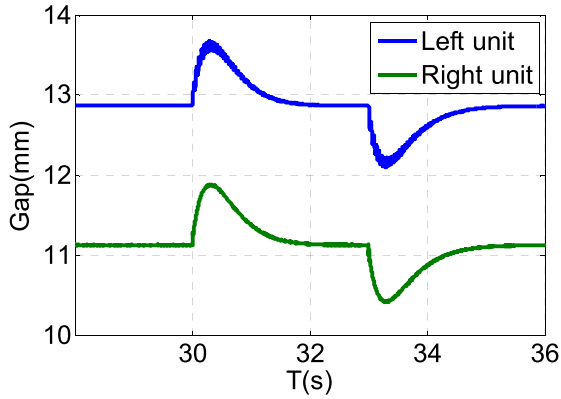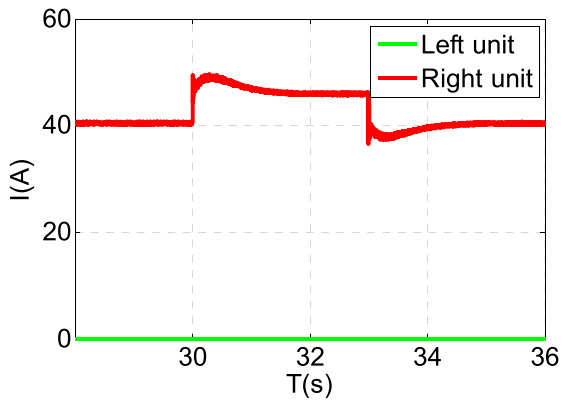
FIGURE 12. The response of suspension join-structure when a step disturbance force of 10kN for 3 seconds on the right unit. (a) The gap of left and right unit. (b) The current of left and right unit.

FIGURE 13. The response of suspension join-structure when a step interference with an amplitude of 2mm for 1 second on the right unit. (a) The gap of left and right unit. (b) The current of left and right unit.

Compared with Eq.12 and Eq.13, it is determined that the matrix A and B are not changed while the matrix C is changed. However, the magnetic levitation system is still completely observable. The state observer is feasible to be established. The system is decomposed in accordance with measurability yields:

$$\begin{pmatrix} \dot{\mathbf{x}}_1 \\ \dot{\mathbf{x}}_2 \end{pmatrix} = \begin{pmatrix} \mathbf{A}_{11} & \mathbf{A}_{12} \\ \mathbf{A}_{21} & \mathbf{A}_{22} \end{pmatrix} \begin{pmatrix} \mathbf{x}_1 \\ \mathbf{x}_2 \end{pmatrix} + \begin{pmatrix} \mathbf{B}_1 \\ \mathbf{B}_2 \end{pmatrix} \mathbf{u} \qquad (14)$$

where $\mathbf{x}_1 = (\dot{c}_{xl} \; c_{xr} \; \dot{c}_{xr})^T$ is measurable, $\mathbf{x}_2 = (c_{xl} \; H \; \dot{H})^T$ is immeasurable and need to be observed. The immeasurable 3-D subsystem state equation is presented as follows:

$$\begin{cases} \dot{\mathbf{x}}_2 = \mathbf{A}_{22}\mathbf{x}_2 + \mathbf{v} \\ \mathbf{z} = \mathbf{A}_{12}\mathbf{x}_2 \end{cases} \qquad (15)$$

The state observer can be designed for this system:

$$\begin{cases} \dot{\hat{\mathbf{x}}}_2 = \mathbf{A}_{22}\hat{\mathbf{x}}_2 + \mathbf{v} + \mathbf{L}(\mathbf{z} - \hat{\mathbf{z}}) \\ \hat{\mathbf{z}} = \mathbf{A}_{12}\hat{\mathbf{x}}_2 \end{cases} \qquad (16)$$

It is believed the poles of the observer depend on the selection of appropriate matrix L. Since the observer has three orders, unlike two-order system, the expected position of the closed-loop poles are not obtained by mathematical

formula. The frequency of the magnetic levitation system is within 20 Hz, and the response time is no shorter than 50 ms. To obtain better dynamic performance, the response time of the observer is adopted as 10 ms. Consequently, the two dominant poles are regulated as $-300 \pm 300i$ and the single-real pole is regulated as -2000. The matrix L of the observer is obtained:

$$\mathbf{L} = \begin{pmatrix} -0.0351 & 0 & 0.0351 \\ 0 & 0 & 0.009 \\ -0.7885 & 0 & 2.1552 \end{pmatrix} \qquad (17)$$

As the Fig. 14 is shown, the response time of the designed observer is no shorter than 10 ms, and satisfy the requirement of magnetic levitation system.

The observation error of the observer is achieved in the Fig. 16. As we can see, the observer is able to estimate the trend change and the error is within a reasonable range.

In order to discuss the effects of sensor failure on the suspension unit when the state observer is designed and used, a series of analysis and investigations are carried out. The following table 2 is summarized.

It is found that both the left suspension unit and the right suspension unit are able to work normally as long as two of the four sensors on the join-structure are valid. When the
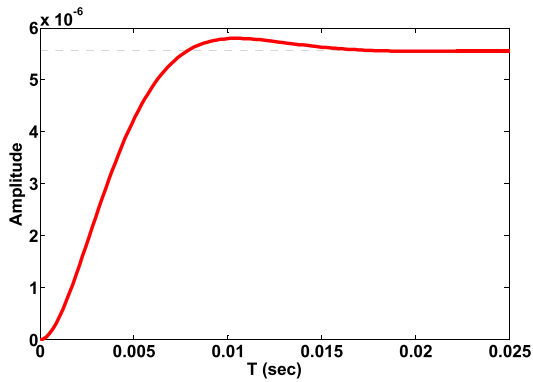
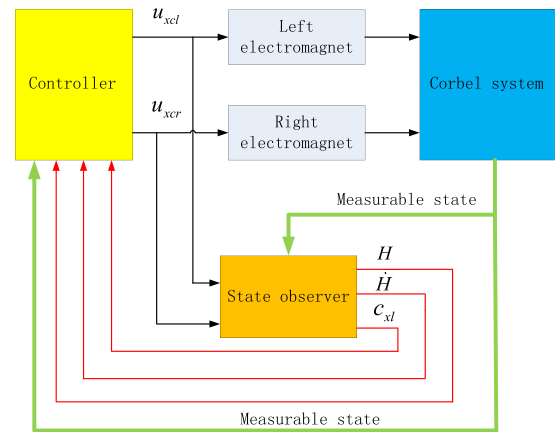**FIGURE 14. Step response curve of the designed observer in three order system.**
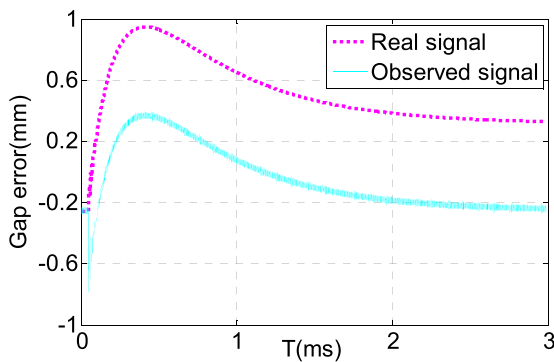

FIGURE 15. The gap errors curve between observed and real.

TABLE 3. The effects of sensor failure on the suspension unit when the state observer is used.

Left side		Right side		Join-structure	
S1	S2	S1	S2	Left unit	Right unit
Y	Y	-	-	Y	Y
Y	-	Y	-	Y	Y
Y	-	-	Y	Y	Y
-	-	Y	Y	Y	Y
-	Y	Y	-	Y	Y
-	Y	-	Y	Y	Y
N	N	N	-	N	N
N	N	-	N	N	N
N	-	N	N	N	N
-	N	N	N	N	N

Y: work; N: failure; -: random

seams are passed, the suspension unit will not break down accordingly.

V. SIMULATION AND VERIFICATION

Based on the designed state observer, the fault-tolerant control system with sensor failure is constructed. The state observer is able to make full use of the measurable signal to estimate the immeasurable gap signal. The suspension controller is able to receive the gap signals and calculate the
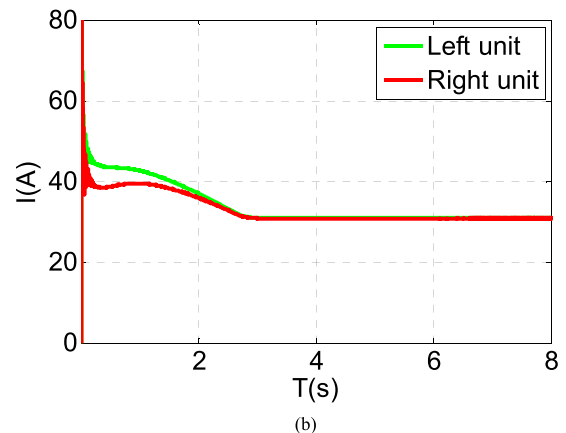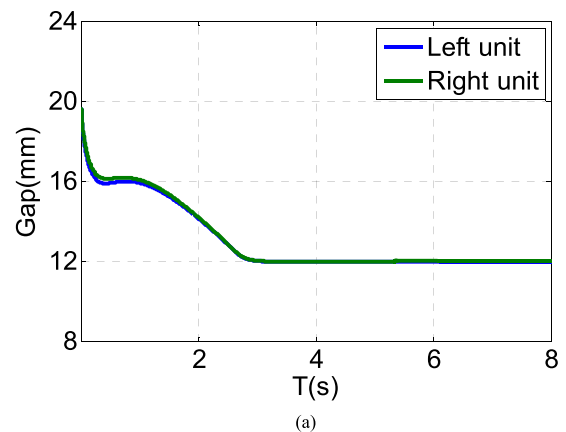

FIGURE 16. The fault-tolerant control system based on state observer.

(a)

(b)

FIGURE 17. The response of suspension join-structure based on state observer when the left gap measurement is invalid. (a) The gap of left and right unit. (b) The current of left and right unit.

control quantity to adjust the position of suspension join-structure.

When the left gap is immeasurable due to the sensor failure, the response of suspension join-structure is observed in Fig. 17.

To illustrate the foregoing analysis and discussion, a great number of significant simulations are performed to have an
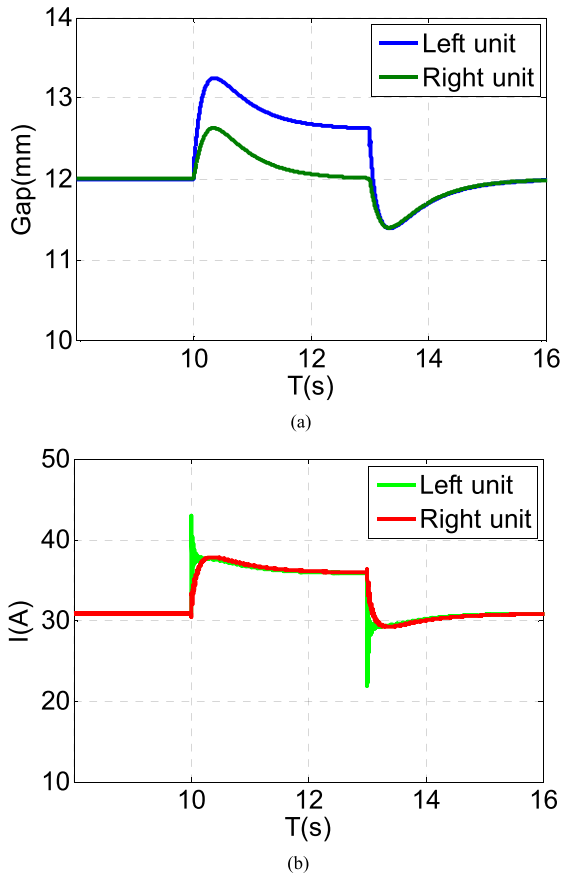
FIGURE 18. The response of suspension join-structure based on state observer when a step disturbance force of 10kN for 3 seconds on the left unit. (a) The gap of left and right unit. (b) The current of left and right unit.

FIGURE 19. The response of suspension join-structure based on state observer when a step disturbance force of 10kN for 3 seconds on the right unit. (a) The gap of left and right unit. (b) The current of left and right unit.

overall evaluation of the fault-tolerant control system based on state observer. In order to test the validity, the same three cases are verified. The system responses in these three cases are described in Fig. 18- Fig. 20.

The performance of fault-tolerant control system based on state observer is examined completely. The investigation carried out by us has achieved plenty of important conclusions:

1. When the left gap measurement is invalid, the left suspension unit will not break down. The left suspension unit and the right suspension unit all work normally in the desired gap.

2. Compared with the modular redundancy strategy, the fluctuation of gap is obviously smaller under the action of disturbance force.

3. The state observer of fault-tolerant control system is set up successfully and the gap measurement is estimated effectively.

The verification demonstrates that the suspension control system based on the established state observer has relatively desirable performance even if disturbed by the external interference. Therefore, the state observer of the suspension control system is set up successfully and the gap measurement is estimated effectively.
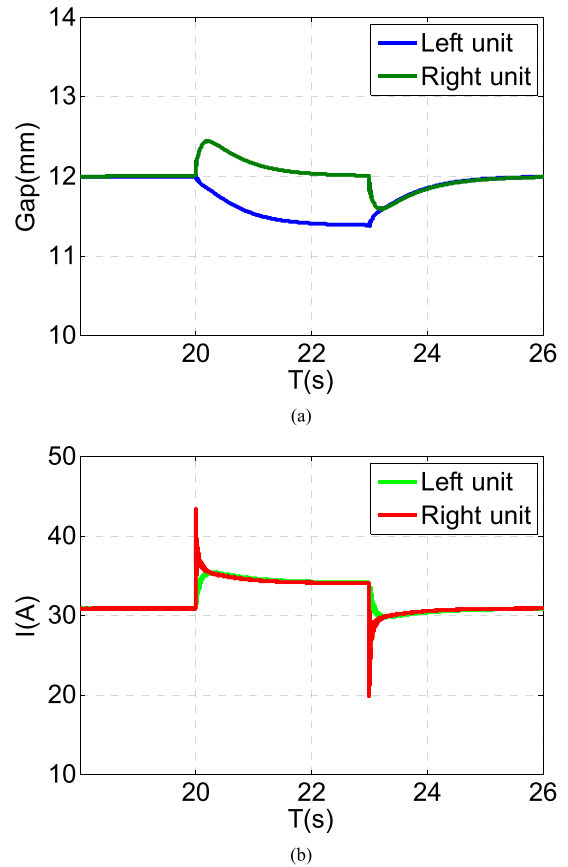
In summary, the redundancy and fault tolerance capacity with sensor failure is significantly improved. on condition that the state observer is established and adopted. The suspension unit will work normally only if two of the four sensors on the join-structure are valid. Although the seams in the track are still existed, the suspension unit will not break down accordingly.

VI. DISCUSSION
When the number of sensors on the join-structure is less two, the suspension will also break down. It is because that the seams are still existed in the track. If only one sensor is valid, the gap measurement will be invalid when the sensor is located below the seam. Therefore, two or more sensors on the join-structure must work normally.

In actual operation, the phenomenon that four or three sensors on the join-structure fail at the same time in one operation interval is very difficult to occur. Therefore, the redundancy and fault tolerance capacity with sensor failure for high speed maglev train is adequate. Moreover, high-speed maglev trains are equipped with diagnostic system, which is able to monitor the working condition of sensors in real time. If one of these sensors fails, the sensor will be replaced in time at the station.

The strategy adopted in this paper is applied without changing the structure of magnetic levitation system. The existing sensors are used to propose and design the fault-tolerant control system based on state observer. In the next study, we can try to change the structure of magnetic levitation system and design the modified sensors to improve the redundancy and fault tolerance capacity of magnetic levitation system with sensor failure.

VII. CONCLUSION

Since National Key R & D Program of China ''maglev traffic system key technology'' was officially established to increase the speed of high speed maglev train up to 600 km/h, the redundancy and fault tolerance of magnetic levitation system, which is considered as the wheels of high-speed maglev train, have always received the most attention from experts and professors. The safety and reliability issues on magnetic levitation system are actually the most critical factors for the high speed maglev train. However, the sensor of magnetic levitation system has a high failure rate since it works at a high-temperature, high-magnetic and high-vibration environment. Because of existence of seams in the track, the suspension unit often breaks down owning to the sensor failure. The performance of suspension join-structure under the modular redundancy strategy for sensor failure was analyzed and investigated. The investigation carried out by us reveals that the overall performance of suspension join-structure is unpleasant and the electromagnet fevers seriously. In order to solve this problem, we propose and design the state observer as a solution to construct the fault-tolerant control system. The designed observer is able to estimate the gap measurement of fault sensor effectively and accurately, so that the suspension unit will not fail due to sensor failure. Therefore, the redundancy and fault tolerance capacity of magnetic levitation system with sensor failure is significantly improved. The fault-tolerant control system based on state observer has relatively desirable performance and solves this problem successfully.

REFERENCES

[1] R. Vickerman, ''High-speed rail and regional development: The case of intermediate stations,'' *J. Transport Geography*, vol. 42, pp. 157–165, Jan. 2015.

[2] H. M. Gutierrez and H. Luijten, ''5-DOF real-time control of active electrodynamic MAGLEV,'' *IEEE Trans. Ind. Electron.*, vol. 65, no. 9, pp. 7468–7476, Sep. 2018.

[3] M. Kim, J.-H. Jeong, J. Lim, M.-C. Won, and C.-H. Kim, ''Design and control of levitation and guidance systems for a semi-high-speed maglev train,'' *J. Electr. Eng. Technol.*, vol. 12, no. 1, pp. 117–125, Jan. 2017.

[4] K. Michail, A. C. Zolotas, and R. M. Goodall, ''Optimised sensor selection for control and fault tolerance of electromagnetic suspension systems: A robust loop shaping approach,'' *ISA Trans.*, vol. 53, no. 1, pp. 97–109, 2014.

[5] S. Chen, G. Liu, and S. Zheng, ''Sensorless control of BLDCM drive for a high-speed maglev blower using low-pass filter,'' *IEEE Trans. Power Electron.*, vol. 32, no. 11, pp. 8845–8856, Nov. 2017.

[6] Z. Gao, C. Cecati, and S. X. Ding, ''A survey of fault diagnosis and fault-tolerant techniques—Part I: Fault diagnosis with model-based and signal-based approaches,'' *IEEE Trans. Ind. Electron.*, vol. 62, no. 6, pp. 3757–3767, Jun. 2015.

[7] Y. Han, D. James Biggs, and N. Cui, ''Adaptive fault-tolerant control of spacecraft attitude dynamics with actuator failures,'' *J. Guid., Control, Dyn.*, vol. 38, no. 10, pp. 2033–2042, Oct. 2015.

[8] S. Yin, H. Luo, and S. X. Ding, ''Real-time implementation of fault-tolerant control systems with performance optimization,'' *IEEE Trans. Ind. Electron.*, vol. 61, no. 5, pp. 2402–2411, May 2014.

[9] Y. A. W. Shardt, H. Hao, and S. X. Ding, ''A new soft-sensor-based process monitoring scheme incorporating infrequent KPI measurements,'' *IEEE Trans. Ind. Electron.*, vol. 62, no. 6, pp. 3843–3851, Jun. 2015.

[10] C. Zou, X. Hu, S. Dey, L. Zhang, and X. Tang, ''Nonlinear fractional-order estimator with guaranteed robustness and stability for lithium-ion batteries,'' *IEEE Trans. Ind. Electron.*, vol. 65, no. 7, pp. 5951–5961, Jul. 2018.

[11] S. Tong, B. Huo, and Y. Li, ''Observer-based adaptive decentralized fuzzy fault-tolerant control of nonlinear large-scale systems with actuator failures,'' *IEEE Trans. Fuzzy Syst.*, vol. 22, no. 1, pp. 1–15, Feb. 2014.

[12] W. Chen, J. Yang, L. Guo, and S. Li, ''Disturbance-observer-based control and related methods-an overview,'' *IEEE Trans. Ind. Electron.*, vol. 63, no. 2, pp. 1083–1095, Feb. 2016.

MINGDA ZHAI received the M.S. degree in control science and engineering from the National University of Defense Technology, Changsha, China, in 2015, where he is currently pursuing the Ph.D. degree in control science and engineering. His research interests include magnetic levitation control, fault diagnosis, tolerant control for maglev trains, and new maglev technology.

ZHIQIANG LONG received the B.S. degree in automation from the Huazhong University of Science and Technology, Wuhan, China, in 1988, the M.S. degree in flight mechanics from the Harbin Institute of Technology, Harbin, China, in 1991, and the Ph.D. degree in control science and engineering from the National University of Defense Technology, Changsha, China, in 2010.

He was with the National University of Defense Technology as a Professor, where he is currently the Head Research Engineer of the Engineering Research Center of Maglev Technology. His research interests include magnetic levitation control, fault diagnosis, tolerant control for maglev trains, and new maglev technology.

XIAOLONG LI received the Ph.D. degree in control science and engineering from the National University of Defense Technology, Changsha, China, in 2009. He was with the National University of Defense Technology as an Associate Research Fellow. His research interests include magnetic levitation control and new maglev technology.

● ● ●